Published in final edited form as:
Dev Biol. 2010 August 15; 344(2): 1035–1046. doi:10.1016/j.ydbio.2010.06.023.

PERICYTE DEFICIENCIES LEAD TO ABERRANT TUMOR VASCULARIZATON IN THE BRAIN OF THE NG2 NULL MOUSE

Feng-Ju Huang[a], **Weon-Kyoo You**[a], **Paolo Bonaldo**[b], **Thomas N. Seyfried**[c], **Elena B. Pasquale**[a], and **William B. Stallcup**[a]

Feng-Ju Huang: fjhuang@burnham.org; Weon-Kyoo You: wyou@burnham.org; Paolo Bonaldo: bonaldo@bio.unipd.it; Thomas N. Seyfried: seyfridt@bc.edu; Elena B. Pasquale: elenap@burnham.org

[a]Sanford-Burnham Medical Research Institute, Cancer Center, 10901 North Torrey Pines Road, La Jolla, CA 92037, USA

[b]University of Padova, Department of Histology, Microbiology, and Medical Biotechnologies, Viale Giuseppe Colombo 3, I-35121, Padova, Italy

[c]Boston College, Higgins Hall, 140 Commonwealth Ave., Chestnut Hill, MA 02467, USA

Abstract

Tightly-regulated crosstalk between endothelial cells and pericytes is required for formation and maintenance of functional blood vessels. When the NG2 proteoglycan is absent from pericyte surfaces, vascularization of syngeneic tumors growing in the C57Bl/6 mouse brain is aberrant in several respects, resulting in retardation of tumor progression. In the NG2 null mouse brain, pericyte investment of the tumor vascular endothelium is reduced, causing deficiencies in both pericyte and endothelial cell maturation, as well as reduced basal lamina assembly. While part of this deficit may be due to the previously-identified role of NG2 in β1 integrin-dependent periyte/endothelial cell crosstalk, the ablation of NG2 also appears responsible for loss of collagen VI anchorage, in turn leading to reduced collagen IV deposition. Poor functionality of tumor vessels in NG2 null brain is reflected by reduced vessel patency and increased vessel leakiness, resulting in large increases in tumor hypoxia. These findings demonstrate the importance of NG2-dependent pericyte/endothelial cell interaction in the development and maturation of tumor blood vessels, identifying NG2 as a potential target for anti-angiogenic cancer therapy.

Keywords

blood vessel maturation; pericyte/endothelial cell interaction; tumor vascularization; tumor progression; NG2 proteoglycan; NG2 null mouse

INTRODUCTION

Tumor progression is affected not only by factors that are intrinsic to the tumor cells themselves, but also by extrinsic factors in the tumor microenvironment. While the importance of oncogenes and other tumor cell-autonomous factors should not be

Corresponding author: William B. Stallcup, Sanford-Burnham Medical Research Institute, 10901 North Torrey Pines Road, La Jolla, CA 92037, (858) 646-3100 x3220, phone (858) 646-3197, fax stallcup@burnham.org.

underestimated, the effects of stromal factors can be surprisingly strong in determining the ability of a tumor to thrive. This has been especially well-documented in the case of breast and ovarian cancer (Roskelley and Bissel, 2002), but also applies to other types of neoplasms. For example, tumorigenesis in the central nervous system is also highly dependent on stromal factors (Rubin, 2008). In addition to contributions from vascular (Plate and Risau, 1995; Fischer et al, 2005) and extracellular matrix elements (Yuan et al, 2007; Delamarre et al, 2009), brain tumor progression can be affected by neural-specific stromal elements such as astrocytes (Couldwell et al, 1992; van der Valk et al, 1997; Duntsch et al, 2005), oligodendrocyte progenitors (Assanah et al, 2006; Ivkovic et al, 2008), and even neural stem cells (Glass et al, 2005; Duntsch et al, 2005).

Perhaps the most universal example of an essential stromal element is the tumor vasculature. Due to the need for gas exchange and access to nutrients, tumor vascularization is required in order for the neoplasm to expand beyond a very small size (Folkman, 1995; Hanahan and Folkman, 1996). The successful recruitment of tumor vasculature is often referred to as the angiogenic switch, the point at which hyperplastic foci acquire the ability to develop into full-blown neoplasms (Folkman et al, 1989; Hanahan and Folkman, 1996; Bergers and Benjamin, 2003; Lin et al, 2006). The ability of an incipient tumor to recruit new blood vessels is critical for its ability not only to grow in size, but also to metastasize to distant sites using blood vessels and lymphatics as conduits. Vascular hyperplasia, involving aggressive recruitment of pericytes and endothelial cells, is a particularly strong characteristic of brain tumors (Assanah et al, 2006; Shibuya, 2009).

The NG2 proteoglycan is a cell surface molecule that has the potential to affect tumor progression both as a tumor cell-autonomous entity and as a component of the tumor vasculature (Stallcup and Huang, 2008). NG2 is commonly found in several types of tumors, notably gliomas (Schrappe et al, 1989; Chekenya and Pilkington, 2002; Shoshan et al, 1999) and melanomas (Campoli et al, 2004; Maciag et al, 2008), and can promote tumor cell proliferation, motility, and resistance to apoptosis (Burg et al, 1997; 1998; Makagiansar et al, 2004; 2007; Chekenya et al, 2008). The proteoglycan is also a prominent component of pericytes in the microvasculature, including tumor microvessels, contributing to pericyte recruitment and to pericyte/endothelial cell interaction (Ozerdem et al, 2001; 2002; Chekenya et al, 2002; Ozerdem and Stallcup, 2003; 2004; Fukushi et al, 2004; Brekke et al, 2006; Tigges et al, 2008).

In order to dissect the respective roles of tumor cell NG2 versus pericyte NG2 in tumor progression, it is necessary to set up experimental systems in which NG2 is expressed only in the host or only in the tumor cells. Both types of analyses are possible using comparisons of wild type and NG2 null mice (Grako et al, 1999; Ozerdem and Stallcup, 2004; Kadoya et al, 2008; Kucharova and Stallcup, 2010) in conjunction with tumor cell lines that are positive or negative for NG2 (Burg et al, 1997; 1998). In this study, we have examined tumors derived by implantation of the NG2-negative melanoma cell line B16F10 (Fidler, 1973), NG2-transfected B16F10 cells (Burg et al, 1998), and the NG2-positive astrocytoma cell line CT2A (Seyfried et al, 2008) in the subcortical white matter of C57Bl/6 wild type and NG2 null mice. Tumors derived from NG2-negative B16F10 cells have been of particular value in the current work, since they allow us to evaluate the tumor promoting effects of stromal NG2 without interference from the effects of tumor cell NG2. This melanoma cell line is a highly relevant model for characterizing tumor growth in the brain, because metastasis to the brain is a frequent occurrence in melanoma progression (Sloan et al, 2009; Guzel et al, 2009). Our results show that NG2 expression by microvascular pericytes is a key factor in the development of a functional vasculature that can support aggressive expansion of tumors growing in the brain. Our results are relevant to normal

development, as well, since pericyte/ endothelial cell interactions are also critical for the development and function of microvessels in normal tissues.

MATERIALS AND METHODS

Cell Lines

NG2-negative B16F10 mouse melanoma cells (American Type Culture Collection; Fidler, 1973), NG2-transfected B16F10 cells (B16F10/NG2; Burg et al, 1998), and NG2-positive CT2A mouse astrocytoma cells (Seyfried et al, 2008) were maintained in Dulbecco's Modified Eagle's Medium (DMEM) containing 10% fetal calf serum, 2 mM glutamine, 100 IU/ml penicillin, and 100 μg/ml streptomycin sulfate. All cells are of C57Bl/6 origin.

Animals

Wild type C57Bl/6 mice, C57Bl/6 NG2 null mice (Grako et al, 1999; Ozerdem and Stallcup, 2004), and C57Bl/6 collagen VI null mice (Bonaldo et al, 1998) were maintained in the Sanford-Burnham Vivarium (fully accredited by the Association for Assessment and Accreditation of Laboratory Animal Care). All animal procedures were performed in accordance with Office of Laboratory Animal Welfare regulations and were approved by Sanford-Burnham Institutional Animal Care and Use Committee review prior to execution.

Cell microinjection and growth of tumors

B16F10, B16F10/NG2, and CT2A cells were harvested by trypsinization and re-suspended in DMEM at a density of 5×10^6 cells/ml. From this suspension, 2 μl (10^4 cells) were microinjected into the forcep minor of the corpus callosum (stereotactic coordinates relative to bregma: 2 mm lateral, 1 mm rostral, 2 mm deep) of male wild type, NG2 null, and collagen VI null mice under Avertin anesthesia. Mice from the three lines were of similar ages and weights (13–15 weeks and 28–32 g). An injection rate of 0.2 μl/minute was maintained by using a Stoelting micropump connected to a 10 μl Hamilton syringe with a 26 gauge needle. Animals were monitored daily for signs of distress, such as weight loss, seizures, posturing, and nasal and/or periorbital hemorrhage. However, these symptoms were never observed during our study. At 3, 5, 7, 11, and 17 days post-injection of B16F10 cells, animals under Avertin anesthesia were perfused with 4% paraformaldehyde, and the brains were removed for analysis. B16F10/NG2 tumors were examined at 11 days post-injection, while CT2A tumors were analyzed at 26 days after injection. Exceptions to this euthanasia regimen were cases in which mice were injected with FITC-dextran, FITC-LEA lectin, or pimonidazole, as described below.

Measurements of tumor size and weight

Brains taken from mice at 17 (B16F10), 11 (B16F10/NG2), or 26 (CT2A) days post-injection were weighed and then photographed using an Olympus SZ2-ILST dissecting light microscope (Tokyo, Japan). After measuring the long and short axes of the tumors, brains were sliced through the midline of the tumor to allow measurement of tumor depth. Tumor volumes were calculated using the formula: $V = 0.52 \times A \times B \times C$, where A is the length of the short axis, B that of the long axis, and C that of tumor depth. Tumor weights (W) were calculated using the formula: $W = M - 0.42g$, where M is the measured weight of brain plus tumor and 0.42g is the average weight of the adult mouse brain.

At 3, 5, 7, and 11 days post-injection, B16F10 tumor volumes were estimated after slicing the brain through the injection site to locate the tumor midline. The pigmentation of the melanoma cells made the tumors readily visible so that the long and short axes could be determined. Tumor volumes were calculated as described above.

Immunohistochemistry, microscopy, and cell counting

In a few cases, brains and tumors were embedded in paraffin, and 10 μm sections prepared for hematoxylin and eosin staining. In most cases, fixed brains were cryoprotected by overnight immersion in 20% sucrose and then frozen in OCT. These blocks were used to prepare 20 μm sections on a Reichert-Jung 1800 cryostat microtome. Immunofluorescence analysis was performed on these sections as described previously (Ozerdem et al., 2001) using the following antibodies: rat anti-CD31 (1:100; BD Biosciences, CA), goat anti-mouse VEGFR2 (1:500, R & D Systems), rabbit anti-PDGFRβ (1:100, Ozerdem et al., 2002), rabbit anti-NG2 (1:100, Ozerdem et al., 2001), mouse anti-smooth muscle actin (1:500; Sigma), rabbit anti-collagen IV and rabbit anti-collagen VI (1/100, Millipore), and Cy5 or FITC-conjugated second antibodies (1:300, Jackson ImmunoResearch, PA). Examination and image capture (TIFF images) from immunostained sections were accomplished using a BioRad (Hercules, CA) inverted Radiance 2100 Multiphoton Confocal Microscope as described previously (Tigges et al., 2008). Serial 1μm optical sections across the entire 20μm thickness of the histological specimens were obtained from 3–5 brains/tumors at each time point. Areas (number of pixels) with immunostaining greater than a set threshold were quantified using computer based morphometry software (Image-Pro Plus 4.5, Diagnostic Instruments, USA).

Determination of vascular leakage

FITC-dextran (250kDa; Sigma) was injected intravenously (100 μl of a 50 mg/ml solution) via the tail vein into Avertin-anesthetized, tumor-bearing mice. After 10 minutes to allow circulation, mice were cervically dislocated while still under anesthesia. Whole brains with tumors were removed without perfusion and fixed overnight in 4% paraformaldehyde. After cryoprotection in 20% sucrose, material was frozen in OCT compound. Cryosections (20 μm) were prepared, and the extent of FITC-dextran leakage from blood vessels was estimated on the basis of green fluorescence located external to CD31-positive vascular structures. Using Image J software, the borders of CD31-labeled blood vessels were identified, so that extravascular FITC-dextran could be quantified by counting green pixels external to red blood vessels. Vascular leakage was defined as total extravascular FITC-dextran per tumor field.

Determination of vascular patency

Functional connection of tumor vessels to the circulation was assessed in Avertin anesthetized mice by tail vein injection of 100 μl of 0.5 mg/ml FITC-labeled *Lysopersicon esculentum* agglutinin (LEA) lectin (Vector Laboratories). After circulation for 3 minutes to allow binding to the vascular endothelium, unbound lectin was cleared by perfusion with saline, followed by perfusion with 4% paraformaldehyde for tissue fixation. Labeling of vessels with FITC-LEA lectin was compared with immunolabeling for CD31 or VEGFR2 as a means of quantifying the percentage of patent vessels.

Determination of tumor hypoxia

Tumor hypoxia was evaluated using a Hypoxyprobe-1 kit (Chemicon International, Temecula, CA). Tumor-bearing mice were injected intraperitoneally with 60 mg/kg pimonidazole hydrochloride and euthanized without perfusion after a 30 minute incubation period. Brains were fixed overnight in 4% paraformaldehyde and then cryoprotected in 20% sucrose. Brains were frozen in OCT, and 20 μm sections were prepared. For visualization of hypoxic areas, sections were incubated overnight with FITC-conjugated Hypoxyprobe antibody. Levels of hypoxia were determined by quantifying green pixels per tumor area.

Statistical analysis

All results were expressed as mean ± SE. Statistical analyses were performed using the two-tailed t test. $P < 0.05$ was considered statistically significant.

RESULTS

Effect of host NG2 ablation on astrocytoma and melanoma growth in the brain

NG2-negative B16F10 melanoma cells, NG2-positive B16F10 melanoma cells (B16F10/NG2), and NG2-positive CT2A astrocytoma cells were microinjected intracranially into the subcortical white matter (corpus callosum) of both wild type and NG2 null mice. For the CT2A studies, 9 wild type and 9 NG2 null recipients were euthanized 26 days after tumor cell injection. Fig. 1A shows that the average CT2A tumor size in NG2 null mice was 7-fold smaller than the average tumor size in wild type mice. Experiments with B16F10/NG2 cells (7 mice in each group) were terminated at 11 days due to rapid growth and invasion of these tumors in the wild type mice. At 11 days, B16F10/NG2 tumors in NG2 null mice were 10-fold smaller than tumors in wild type mice (Fig.1B). For the B16F10 studies, cohorts of mice were euthanized at 3, 5, 7, 11, and 17 days post-injection to allow examination of tumor progression. Even in the case of very small early tumors, the pigmentation of the B16F10 cells makes it straightforward to determine tumor boundaries and to quantify tumor sizes. A plot of tumor sizes as a function of time (Fig. 1C) reveals that tumors in wild type and NG2 null mice begin to diverge in volume between days 3 and 7 post-injection (inset panel), and that this difference has become quite large at 17 days post-injection. At 17 days, tumors in NG2 null mice are roughly one-third the size of tumors in wild type mice (Fig. 1D). Thus, in the case of all three cell lines, the NG2 negative host background is responsible for reduced tumor progression.

In all three tumors growing in wild type mice, NG2 is expressed by pericytes associated with CD31-positive endothelial cells in tumor blood vessels (Fig. 1E shows this for the B16F10 and B16F10/NG2 tumors). Fig. 1E also demonstrates the expression of NG2 by B16F10/NG2 cells (also true for CT2A cells, data not shown) and the absence of NG2 from B16F10 cells. In order to focus on the stromal role of NG2 in tumor progression, we devoted our attention to the B16F10 tumors for the remainder of this study. The role of tumor cell NG2 in neoplastic progression (for example, in the case of B16F10/NG2 and CT2A cells) will be the subject of future studies. This is clearly a topic of interest in light of the extremely aggressive growth and invasion seen with B16F10/NG2 tumors.

Effect of host NG2 ablation on pericyte/endothelial cell interaction

Since NG2 is not expressed by the B16F10 tumor cells in our model, stromal elements must be responsible for the effects of NG2 ablation on B16F10 tumor progression. In the context of the central nervous system, NG2 is expressed by oligodendrocyte progenitor cells, by macrophages/microglia, and by microvascular pericytes (Stallcup and Huang, 2008). Leaving the former two cell types for future investigation, we have focused our initial attention on pericytes in the tumor vasculature. Our previous work using pathological retinal and corneal models has demonstrated reduced neovascularization in the NG2 null mouse (Ozerdem and Stallcup, 2004). This decrease stems largely from deficiencies in pericyte recruitment and from loss of NG2-dependent pericyte interaction with endothelial cells (Fukushi et al, 2004). To look for evidence of changes in pericyte recruitment and/or pericyte/endothelial cell interaction in B16F10 tumors, we collected tumor specimens at day 7 following intracranial injection. This time point offers the advantage of providing samples that are large enough to allow preparation of multiple histological sections, but small enough to avoid problems with necrosis that become common at later stages. For example in day 11

tumors, not only is necrosis a significant factor, but many vessels also begin to exhibit extreme dilation that makes straightforward analysis difficult.

Using the day 7 tumor specimens from wild type and NG2 null brains, we did not detect significant differences in either microvascular density or vessel diameter (data not shown). We also did not find differences in the absolute numbers of pericytes present in the two sets of tumors (Fig. 2A, B). However, double staining for the endothelial cell marker CD31 and the NG2-independent pericyte marker platelet-derived growth factor beta-receptor (PDGFRβ revealed clear differences in the relationship between these two cell populations. Compared to wild type hosts, NG2 null hosts exhibited an increased number of pericytes lacking physical association with CD31-positive endothelial tubes (Fig. 2A, C), suggesting a role for NG2 in mediating pericyte/endothelial cell interaction. Moreover, there was a difference in the extent of pericyte coverage of endothelial tubes in the two sets of tumors. Since CD31 and PDGFRβ are present on distinct cell populations, they cannot overlap with each other in a single optical section. However, because pericytes form an intricate ensheathment of endothelial cells, the two labels appear to overlap when viewed in 3-dimensional space. Analysis of z-stacks of confocal images (Fig. 2A) therefore allowed us to quantify the extent to which PDGFRβ labeling overlapped with CD31 labeling. The percentage of the CD31 area with pericyte ensheathment was reduced two-fold in tumor vessels in the NG2 null mouse (Fig. 2D). Very similar reductions in pericyte ensheathment were seen when endosialin antibodies (MacFadyen et al, 2007; Simonavicius et al, 2008) were used to label pericytes (data not shown), verifying that the result is independent of the choice of marker. Although the magnitude of investment was lower, this difference in the pericyte ensheathment of endothelial cells in wild type and NG2 null mice was also detectable in day 5 tumors, representing an intermediate stage of vessel development during which pericytes are first becoming evident (Fig.2D).

Effects of host NG2 ablation on pericyte maturation

The interaction between pericytes and endothelial cells has profound consequences for the maturation and function of both of these cell types (Bergers and Song, 2005; Betsholtz et al, 2005; Gaengel et al, 2009). For example, the reduced pericyte ensheathment of endothelial cells observed in tumor vessels in NG2 null mice results in a pronounced decrease in pericyte maturation. This conclusion is based on quantification of pericyte expression of α-smooth muscle actin (αSMA), a marker that is largely absent from nascent murine pericytes but which is up-regulated as these cells mature (Ozerdem et al, 2001; 2002; Song et al, 2005; Hamzah et al, 2008). Double-labeling for PDGFRβ and αSMA (Fig. 2E) shows that a portion of the PDGFRβ-positive pericytes in wild type tumor vessels have begun to express αSMA after 7 days of tumor development. In contrast, very little αSMA expression is seen in PDGFRβ-positive pericytes in NG2 null tumor vessels at this time point. Quantification of the dual expression of these two markers reveals a ten-fold decrease in αSMA expression by NG2 null pericytes (Fig. 2F).

Effects of host NG2 ablation on basal lamina deposition

The effect of pericyte/endothelial cell interaction on endothelial cells is reflected, in part, by deposition of the subendothelial basement membrane, a critical step in vessel maturation. Although production of the major extracellular matrix elements involved in basement membrane assembly has been largely attributed to the vascular endothelium, it is clear that pericyte investment of endothelial cells is required for effective basal lamina deposition (Kalluri, 2003; Davis and Senger, 2005). We have used an antibody against collagen IV, the predominant collagen species present in vascular basement membranes, to assess basal lamina deposition associated with tumor vessels in specimens at the 7-day time point. This analysis demonstrated a large decrease in collagen IV deposition associated with tumor

vessels in NG2 null hosts (Fig. 3A). Image analysis of the overlap between collagen IV labeling and CD31 labeling revealed a 4-fold decrease in collagen IV deposition in the absence of NG2 (Fig. 3B). Even at 5 days, when pericyte ensheathment of endothelial cells is in its early stages, a deficiency in collagen IV-positive basement membrane assembly is already detectable in the NG2 null tumors (Fig. 3B), probably as a result of reduced pericyte/endothelial cell interaction.

The effect of NG2 on collagen IV deposition might be an indirect one in which the proteoglycan is necessary for mediating the pericyte/endothelial cell interaction that promotes basal lamina deposition (Davis and Senger, 2005). We have shown that NG2-dependent activation of β1 integrin signaling in endothelial cells (Fukushi et al, 2004) provides the basis for this pericyte/endothelial cell interaction. In addition, NG2 might also have a more direct role in mediating collagen IV deposition. A possible mechanism for this scenario is suggested by the fact that NG2 is a cell surface ligand for collagen VI (Stallcup and Huang, 2008). In turn, collagen VI has been demonstrated as a binding partner for collagen IV (Kuo et al, 1998). Thus the absence of NG2 could result in decreased collagen VI deposition, leading to loss of anchorage for collagen IV. Analysis of B16F10 tumors in wild type and NG2 null mice indeed reveals a large decrease in vascular collagen VI deposition in the null mice (Fig. 3C). In the absence of NG2, collagen VI deposition relative to CD31 labeling is reduced by almost 3-fold (Fig. 3D). Further evidence for the importance of collagen VI deposition is provided by examination of B16F10 tumors implanted in collagen VI null mice. If collagen VI anchorage to NG2 is necessary for collagen IV deposition, then we should also find reduced deposition of collagen IV in B16F10 tumor vessels in the collagen VI null mouse. As predicted, collagen IV deposition is reduced in the collagen VI null mouse to an even larger degree (4-fold) than in the NG2 null mouse (Fig. 3E). These observations are consistent with a model in which NG2 is needed for collagen VI anchorage, with collagen VI in turn providing a scaffold for assembly of the collagen IV-containing basal lamina.

Effects of host NG2 ablation on vessel function

The observed deficits in pericyte coverage, pericyte maturation, and basal lamina deposition in the tumor vessels of the NG2 null mouse might be expected to have negative effects on vessel function. To investigate this possibility, we used perfusion with FITC-LEA lectin to examine vessel patency, and perfusion with FITC-dextran to examine vessel leakiness. As stated above, we did not observe a difference in the number of CD31-positive vessels between tumors growing in wild type and NG2 null mice. However, intravenous injection of FITC-LEA lectin, followed by saline perfusion to remove lectin that was not bound to endothelial cells, reveals that 7 day tumors in NG2 null mice have decreased numbers of VEGFR2-positive vessels that are perfused by the circulation (Fig. 4A). Whereas almost all tumor vessels are patent in wild type mice, only 50% of the tumor vessels are patent in NG2 null mice (Fig. 4B).

In addition, intravenous injection of FITC-dextran (250 kDa) shows that patent tumor vessels in NG2 null hosts are considerably leakier at 7 days than tumor vessels in wild type hosts (Fig. 5A, lower panels). Quantification of the percentage of FITC-dextran located external to CD31-positive vessels reveals a 4-fold increase in tumor vessel leakiness in the NG2 null mouse (Fig. 5B, right panel). Interestingly, after 3 days of tumor development, vessels in both wild type and NG2 null hosts exhibit a high level of leakage (Fig. 5A, top panels and Fig. 5B, left panel; note the contrast in leakage between tumor vessels and vessels outside the tumor). This is likely attributable to the fact that pericyte investment of endothelial tubes in the tumors is absent at day 3 (Fig. 5C), affecting vessel permeability in both sets of hosts. At day 5, even though pericyte/endothelial cell interaction in wild type mice is superior to that in NG2 null mice (Figure 2D), pericyte ensheathment is nevertheless

at an early stage, so that vessels are still leaky in both sets of tumor vessels (data not shown). The development of an effective pericyte investment and basal lamina in wild type hosts between days 3 and 7 may be the primary reason why tumor growth in these animals diverges from tumor growth in NG2 null animals during this time period.

Effect of host NG2 ablation on tumor hypoxia

To further compare tumor vessel functionality in wild type and NG2 null mice, we injected a pimonidazole hypoxia probe, followed by immunocytochemistry to quantify the extent of local hypoxia. At 3 days of tumor development, tissue hypoxia is low in both wild type and NG2 null mice, despite the leakiness of tumor vessels in both cases (Fig. 6A, B). The extremely small size of these tumors may allow them access to gases and nutrients even in the absence of an efficient vasculature. After 7 days of tumor growth, however, high levels of hypoxia are evident in tumors from NG2 null mice. In contrast, tumors in wild type mice exhibit 20-fold lower levels of hypoxia (Fig. 6C, D).

DISCUSSION

Since blood vessels are critical elements of the tumor microenvironment, mechanisms responsible for the recruitment and development of vascular components are of key importance to our understanding of tumor progression and to our attempts to manipulate this process. Of the two primary vascular cell types, vascular endothelial cells have traditionally received the most attention in studies of blood vessel development. However, it is clear that perivascular cells (pericytes) also are required for establishment and maintenance of a functional vasculature (Betsholtz et al, 2005; Bergers and Song, 2005; Hall, 2006; Gaengel et al, 2009). In addition to stabilization of endothelial tubes, pericytes play much earlier roles in neovascularization than previously suspected (Schlingemann et al, 1990;1996; Nehls et al 1992; Wesseling et al, 1995; Redmer et al, 2001; Ozerdem et al, 2001; 2002; Ozerdem and Stallcup, 2003; Song et al, 2005; Virgintino et al, 2007). Recognition of this important, early role of pericytes in blood vessel development is due in part to the use of markers such as PDGFRβ and NG2 proteoglycan that permit identification of perivascular cells at early time points in their development. By contrast, the use of markers such as αSMA often fails to reveal the early involvement of pericytes in microvessel development, due to the fact that αSMA is expressed by mature rather than nascent pericytes.

While the importance of PDGFRβ signaling in pericyte recruitment and development has been well documented (Lindahl et al, 1997; Lindahl and Betsholtz, 1998; Hellstrom et al, 1999; 2001; Enge et al, 2002), the role of NG2 in pericyte biology is just beginning to emerge. In a number of different cell types, NG2 has been shown to promote proliferation and motility (Burg et al, 1997, 1998; Grako and Stallcup, 1995; Grako et al, 1999; Makagiansar et al, 2004; 2007; Kadoya et al, 2008; Kucharova and Stallcup, 2010), suggesting that genetic ablation of NG2 might have a negative effect on pericyte recruitment. Recruitment deficits resulting from NG2 ablation have been documented most clearly in models of retinal neovascularization in response to ischemia, and corneal neovascularization in response to FGF2 (Ozerdem and Stallcup, 2004). In both cases, pericyte recruitment is severely compromised in the NG2 null mouse, resulting in reduced establishment of new blood vessels. Other studies from our group have provided indications that NG2 not only affects pericyte recruitment, but also is able to mediate pericyte/endothelial cell interaction. NG2 interacts physically with β1 integrins and can promote β1 integrin activation in both *cis* and *trans* settings, i.e. with the two molecules expressed either on the same cell or on neighboring cells (Fukushi et al, 2004; Makagiansar et al, 2004, 2007; Chekenya et al, 2008). Thus, in the case of pericyte/endothelial cell interaction, NG2 expressed by pericytes can activate β1 integrin signaling in endothelial cells, promoting endothelial cell recruitment and morphogenesis (Fukushi et al, 2004). Ablation of NG2

would therefore be expected to have a negative effect on pericyte/endothelial cell interaction.

The fact that genetic ablation of NG2 causes reduced neovascularization in both corneal and retinal models (Ozerdem and Stallcup, 2004) suggests that tumor vascularization and tumor growth might also be reduced in the NG2 null mouse. In fact, two brief reports have demonstrated reduced microvascular densities in transplanted prostate (Ozerdem, 2006a) and uveal melanoma tumors (Ozerdem, 2006b) grown in NG2 null mice. In our current work, we have examined this question in more depth using engraftment of NG2-negative and NG2-positive B16F10 melanoma cells, and also NG2-positive CT2A astrocytoma cells into the subcortical white matter of wild type and NG2 null mouse brains to evaluate the importance of NG2 in the microenvironment of brain tumors. While studying the growth of human tumor cell lines in immune compromised hosts remains an option for the future, evaluating the progression of the C57Bl/6 tumors in syngeneic, immune competent recipients permits us to examine all aspects of the tumor microenvironment, including elements of the host immune/inflammatory response.

Our results show that tumor progression by both astrocytoma cells (CT2A) and melanoma cells (B16F10 and B16F10/NG2) is greatly retarded in NG2 null hosts. In the case of CT2A and B16F10/NG2 tumors, mechanistic interpretations of these phenomena are complicated by the presence of NG2 not only in the tumor stroma, but also on the tumor cells themselves, possibly contributing to tumor cell proliferation and invasion. However, since NG2 is not expressed by the tumor cells in the B16F10 model, stromal elements must be responsible for these effects of NG2 ablation on tumor progression. In addition to its expression in the vasculature, NG2 can also be found on other components of the tumor microenvironment. In the context of the central nervous system, NG2 is expressed by oligodendrocyte progenitors and by macrophages/microglia (Stallcup and Huang, 2008), both of which can contribute to brain tumor progression. Leaving these latter two cell types for future investigation, we have focused our initial attention on pericytes in the B16F10 tumor blood vessels. In the NG2 null mouse, the extent of pericyte ensheathment of the tumor vascular endothelium is reduced two-fold compared to that seen in the wild type mouse. This is true during the early stages of pericyte/endothelial cell interaction (day 5) as well as in more mature vessels (day 7), suggesting that the primary effect of NG2 ablation in this model is on the quality of the interaction that occurs between pericytes and endothelial cells. This is consistent with our expectation that NG2 ablation should negatively affect pericyte-dependent activation of β1 integrin signaling in endothelial cells, resulting in loss of crosstalk between the two cell populations (Fukushi et al, 2004).

The relatively modest two-fold decrease in pericyte ensheathment of endothelial cells observed in the NG2 null mouse brain has rather dramatic effects on vessel maturation and function. The developmental programs of both pericytes and endothelial cells are affected by the interaction between the two cell types, and maturation of both cell types is negatively impacted by the decreased pericyte ensheathment of endothelial cells seen in the NG2 null mouse. In the case of pericytes, we find that expression of the maturation marker αSMA is drastically curtailed due to reduced pericyte/endothelial cell interaction in the absence of NG2. In the case of endothelial cells, impaired interaction between endothelial cells and NG2 null pericytes leads to severely compromised ability of the endothelial cells to assemble the vascular basal lamina (as judged by a 2 to 4-fold decrease in collagen IV deposition at days 5 and 7, respectively). The deposition of this subendothelial basement membrane is one of the most important consequences of the pericyte/endothelial cell collaboration, since it serves to stabilize the maturing vessel. In the B16F10 model at days 5 and 7, assembly of the collagen IV-positive basal lamina appears to proceed in parallel with pericyte ensheathment of endothelial cells. In addition to its β1 integrin-dependent role in

pericyte/endothelial cell crosstalk, (Fukushi et al, 2004), NG2 also appears capable of exerting a more direct effect on basal lamina deposition by acting as a cell surface receptor for collagen VI (Stallcup et al, 1990; Nishiyama and Stallcup, 1993; Burg et al, 1996, 1997; Tillet et al, 1997, 2002). Collagen VI serves as a linker between cell surface receptors (such as NG2) and other fibrillar collagen species, including collagen IV (Kuo et al, 1997), involved in assembly of extracellular matrices and basement membranes. Ablation of NG2 thus reduces the anchorage of collagen VI to the cell surface, which in turn eliminates a nucleation point for assembly of the collagen IV-containing basal lamina.

Functional consequences of these deficits in vessel maturation in the NG2 null mouse include decreased patency of B16F10 tumor vessels, as judged by perfusion with FITC-LEA lectin, and increased leakiness of vessels that are perfused by the circulation, as detected by vascular loss of intravenously injected FITC-dextran. The decrease in tumor vessel leakiness seen in wild type mice between days 3 and 7 of tumor development coincides with the development of pericyte ensheathment. At 3 days of tumor development, vessels have not yet acquired a pericyte investment, and at 5 days ensheathment is incomplete. At these time points, vessels are permeable to FITC-dextran in both wild type and NG2 null mice. However, by 7 days, pericyte-ensheathed tumor vessels in wild type mice are dramatically less leaky, while significant FITC-dextran leakage is still seen in NG2 null mice. Probably as a result of both poor vessel patency and increased vessel leakiness, tumors in NG2 null mice exhibit 20-fold higher levels of hypoxia than tumors in wild type mice. In NG2 null mice, the failure to develop an effective pericyte investment, the continuing vessel leakiness, and the development of high levels of tissue hypoxia all occur during the same time period (days 3–7) when tumor growth in these animals diverges from the more rapid growth observed in wild type mice. These observations suggest a causal relationship between vessel performance and tumor progression. These effects of NG2 ablation are not restricted to tumors growing in the brain. In addition to reduced vascularization of prostate (subcutaneous) and uveal melanoma (cornea) xenografts in the NG2 null mouse (Ozerdem, 2006a,b), work in progress in our laboratory shows that NG2 ablation in the context of the MMTV-PyMT transgenic mouse model (Lin et al, 2003) greatly slows mammary tumor progression. Since NG2 is not expressed by mammary tumor cells in this model, the effects of NG2 ablation must come from the tumor stroma. Using the same methodology described in this report, we detect deficits in pericyte/endothelial cell interaction in mammary tumor vessels of the NG2 null mouse, leading to reduced basal lamina deposition and to high levels of tumor hypoxia (our unpublished data).

The consequences of NG2 ablation on tumor vascularization are in dramatic contrast to the results of knocking out another pericyte-specific marker, regulator of G-protein signaling 5 (Rgs5). Compared to tumor vessels in wild type mice, tumor vessels in Rgs5-deficient mice exhibit a normalized morphology and reduced leakiness, resulting in decreased tissue hypoxia and enhanced tumor growth (Hamzah et al, 2008). These contrasting results undoubtedly reflect the different roles that NG2 and Rgs5 play in pericyte biology, although both of these roles remain incompletely understood. Rgs5 appears to inhibit vessel maturation, so that its ablation allows maturation to occur. On the other hand, we show here that NG2 is important for pericyte/endothelial cell interaction and vessel maturation, so that its ablation interferes with the maturation process. Since pericyte/endothelial cell interactions are fundamental to all types of vascularization models, these findings have relevance that extends far beyond the specific example of tumor vascularization studied in the current work.

In future investigations, we will seek additional details concerning the mechanisms underlying this vascular role of NG2. In addition, we will further examine the important role of NG2 in the proliferative and invasive properties of the tumor cells themselves. Previous

work has indicated that tumor cell NG2 has important effects on both melanoma and glioma progression (Burg et al, 1998; Chekenya et al, 2008). However, these studies were not designed to dissect the respective contributions of tumor cell NG2 and stromal NG2. The very large growth discrepancy in wild type versus NG2 null mice seen in our current study with NG2-positive tumor cells (B16F10/NG2 and CT2A) suggest that there might be a synergistic effect between tumor cell and stromal NG2. Orthotopic transplantations in NG2 null mice using the B16F10 and B16F10/NG2 cells will be able to identify the specific effects of tumor cell NG2 on tumor progression. The multifunctional nature of NG2 and its expression by both tumor and stromal cell types make the proteoglycan an intriguing target for cancer therapy (Campoli et al, 2004; Maciag et al, 2008; Chekenya et al, 2008).

Acknowledgments

This work was supported by R01 CA95287 (WBS), P01 HD25938 (WBS and EBP), and P30 CA30199 (pilot project award to WBS and EBP). We thank Dr. Clare Isacke for the generous gift of antibodies against endosialin, Dr. Masanobu Komatsu for helpful discussions, and Ms. Regina Kapono for assistance with the manuscript. The authors have no conflicting financial interests. Funding sources had no involvement in the study design, conduct of the research, or preparation of the manuscript.

References

Assanah M, Lochhead R, Ogden A, Bruce J, Goldman J, Canoll P. Glial progenitors in adult white matter are driven to form malignant gliomas by platelet-derived growth factor-expressing retroviruses. J Neurosci. 2006; 26:6781–6790. [PubMed: 16793885]

Bergers G, Benjamin L. Tumorigenesis and the angiogenic switch. Nature Rev Cancer. 2003; 3:401–410. [PubMed: 12778130]

Bergers G, Song S. The role of pericytes in blood vessel formation. Neurooncol. 2005; 7:452–464.

Betsholtz C, Lindblom P, Gerhardt H. Role of pericytes in vascular morphogenesis. EXS. 2005; 94:115–125. [PubMed: 15617474]

Bonaldo P, Braghetta P, Zanetti M, Piccolo S, Volpin D, Bressan G. Collagen VI deficiency induces early onset myopathy in the mouse: an animal model for Bethlem myopathy. Hum Mol Genet. 1998; 7:2135–2140. [PubMed: 9817932]

Brekke C, Lundervold A, Enger P, Brekken C, Stalsett E, Pedersen T, Haraldseth O, Kruger P, Bjerkvig P, Chekenya M. NG2 expression regulates vascular morphology and function in human brain tumors. NeuroImage. 2006; 29:965–976. [PubMed: 16253523]

Burg MA, Tillet E, Timpl R, Stallcup WB. Binding of the NG2 proteoglycan to type VI collagen and other extracellular matrix molecules. J Biol Chem. 1996; 271:26110–26116. [PubMed: 8824254]

Burg MA, Nishiyama A, Stallcup WB. A central segment of the NG2 proteoglycan is critical for the ability of glioma cells to bind and migrate toward type VI collagen. Exp Cell Res. 1997; 235:254–264. [PubMed: 9281375]

Burg MA, Grako KA, Stallcup WB. Expression of the NG2 proteoglycan enhances the growth and metastatic properties of melanoma. J Cell Physiol. 1998; 177:299–312. [PubMed: 9766527]

Campoli M, Chang C, Kageshita T, Wang X, McCarthy J, Ferrone S. Human high molecular weight melanoma associated antigen (HMW-MAA): a melanoma cell surface chondroitin sulfate proteoglycan (MSCP) with biological and clinical significance. Crit Rev Immunol. 2004; 24:267–296. [PubMed: 15588226]

Chekenya M, Pilkington G. NG2 precursor cells in neoplasia: functional, histogenesis, and therapeutic implications for malignant brain tumors. J Neurocytol. 2002; 31:507–521. [PubMed: 14501220]

Chekenya M, Hjelstuen M, Enger P, Thorsen F, Jacob A, Probst B, Haraldseth O, Pilkington G, Butt A, Levine J, Bjerkvig R. NG2 proteoglycan promotes angiogenesis-dependent tumor growth in CNS by sequestering angiostatin. FASEB J. 2002; 16:586–588. [PubMed: 11919162]

Chekenya M, Krakstad C, Svendsen A, Sakarisassen P, Tysnes B, Staalesen V, Seilheim F, Wang J, Sandal T, Flatmark T, Lonning P, Enger P, Bjerkvig R, Sioud M, Stallcup WB. The progenitor cell marker NG2/HMP promotes chemoresistance by activation of integrin/PI3K/Akt signaling. Oncogene. 2008; 27:5182–5194. [PubMed: 18469852]

Couldwell W, Fraser G, de Vellis G, et al. Malignant glioma-derived soluble factors regulate proliferation of normal adult human astroctes. J Neuropathol Exp Neurol. 1992; 51:506–513. [PubMed: 1517771]

Davis GE, Senger DR. Endothelial extracellular matrix. Biosynthesis, remodeling, and functions during vascular morphogenesis and neovessel stablization. Circ Res. 2005; 97:1093–1107. [PubMed: 16306453]

Delamarre E, Taboubi S, Mathieu S, Berenguer C, Rigot V, Lissitzki J, Figarella-Branger D, Ouafik L, Luis J. Expression of integrin alpha-6, beta-1 enhances tumorigenesis in glioma cells. Am J Pathol. 2009; 175:844–855. [PubMed: 19574430]

Duntsch C, Zhou Q, Weimar J, Frankel B, Robertson J, Pourmotabbed T. Up-regulation of neuropoiesis generating glial progenitors that infiltrate rat intracranial glioma. J Neurooncol. 2005; 71:245–255. [PubMed: 15735912]

Enge M, Bjarnegard M, Gerhardt H, Gustafsson E, Kalen M, Asker N, Hammes H, Shan M, Fassler R, Bestsholtz C. Endothlium-specific platelet-derived growth factor-B ablation mimics diabetic retinopathy. EMBO J. 2002; 21:4307–4316. [PubMed: 12169633]

Fidler IS. Selection of successive tumor lines for metastasis. Nature. 1973; 242:148–149.

Fischer I, Gagner JP, Law M, Newcomb EW, Zagzag D. Angiogenesis in gliomas: biology and molecular pathophysiology. Brain Pathol. 2005; 15:297–310. [PubMed: 16389942]

Folkman J. Angiogenesis in cancer, vascular, rheumatoid, and other disease. Nature Med. 1995; 1:27–31. [PubMed: 7584949]

Folkman J, Watson K, Ingber D, Hanahan D. Induction of angiogenesis during the transition from hyperplasia to neoplasia. Nature. 1989; 339:58–61. [PubMed: 2469964]

Fukushi J, Makagiansar I, Stallcup WB. NG2 proteoglycan promotes endothelial cell motility and angiogenesis via engagement of galectin-3 and α3β1 integrin. Mol Biol Cell. 2004; 15:3580–3590. [PubMed: 15181153]

Gaengel K, Genove G, Armulik A, Betsholtz C. Endothelial-mural cell signaling in vascular development and angiogenesis. Arterioscler Thromb Vasc Biol. 2009; 29:630–638. [PubMed: 19164813]

Glass R, Synowitz M, Kronenberg G, Walzlein J, Markovic D, Wang J, Gast D, Kiwit J, Kempermann G, Kettenmann H. Glioblastoma-induced attraction of endogenous neural precursor cells is associated with improved survival. J Neurosci. 2005; 25:2637–2646. [PubMed: 15758174]

Grako K, Stallcup WB. Participation of the NG2 proteoglycan in rat aortic smooth muscle cell responses to platelet-derived growth factor. Exp Cell Res. 1995; 221:231–240. [PubMed: 7589250]

Grako KA, Ochiya T, Barritt D, Nishiyama A, Stallcup WB. PDGF alpha-receptor is unresponsive to PDGF-AA in aortic smooth muscle cells from the NG2 knockout mouse. J Cell Sci. 1999; 112:905–915. [PubMed: 10036240]

Guzel A, Maciaczyk J, Dohmen-Scheuffler H, Senturk S, Volk B, Ostertag C, Nikkhah G. Multiple intracranial melanoma metastases: a case report and review of the literature. J Neurooncol. 2009; 93:413–420. [PubMed: 19184642]

Hall A. Review of the pericyte during angiogenesis and its role in cancer and diabetic retinopathy. Toxicol Pathol. 2006; 34:763–775. [PubMed: 17162534]

Hamzah J, Jugold M, Kiessling F, Rigby P, Manzur M, Marti H, Rabie T, Kaden S, Grone HJ, Hammerling G, Arnold B, Ganss R. Vascular normalization in Rgs5-deficient tumors promotes immune destruction. Nature. 2008; 453:410–414. [PubMed: 18418378]

Hanahan D, Folkman J. Patterns and emerging mechanisms of the angiogenic switch during tumorigenesis. Cell. 1996; 86:353–364. [PubMed: 8756718]

Hellstrom M, Kalen M, Lindahl P, Abramsson A, Betsholtz C. Role of PDGF-B and PDGFR-beta in recruitment of vascular smooth muscle cells and pericytes during embryonic blood vessel formation in the mouse. Development. 1999; 126:3047–3055. [PubMed: 10375497]

Hellstrom M, Gerhardt H, Kalen M, Li X, Eriksson U, Wolburg H, Betsholtz C. Lack of pericytes leads to endothelial hyperplasia and abnormal vascular morphogenesis. J Cell Biol. 2001; 153:543–553. [PubMed: 11331305]

Ivkovic S, Canoll P, Goldman J. Constitutive EGFR signaling in oligodendrocyte progenitors leads to diffuse hyperplasia in postnatal white matter. J Neurosci. 2008; 28:914–922. [PubMed: 18216199]

Kadoya K, Fukushi J, Matsumoto Y, Yamaguchi Y, Stallcup WB. NG2 proteoglycan expression in mouse skin: altered postnatal skin development in the NG2 null mouse. J Histochem Cytochem. 2008; 56:295–303. [PubMed: 18040080]

Kalluri R. Basement membranes: structure, assembly, and role in tumour angiogenesis. Nature Rev Cancer. 2003; 3:422–433. [PubMed: 12778132]

Kucharova K, Stallcup WB. The NG2 proteoglycan promotes oligodendrocyte progenitor proliferation and developmental myelination. Neuroscience. 2010; 166:185–194. [PubMed: 20006679]

Kuo H, Maslen C, Keene D, Glanville R. Type VI collagen anchors endothelial basement membranes by interacting with type IV collagen. J Biol Chem. 1997; 272:26522–26529. [PubMed: 9334230]

Lin E, Jones J, Li P, Zhu L, Whitney K, Muller W, Pollard J. Progression to malignancy in the polyoma middle T oncoprotein mouse breast cancer model provides a reliable model for human diseases. Am J Pathol. 2003; 163:2113–2126. [PubMed: 14578209]

Lin E, Li J, Gnatovski L, Deng Y, Zhu L, Grzesik D, Qian H, Xue X, Pollard J. Macrophages regulate the angiogenic switch in a mouse model of breast cancer. Cancer Res. 2006; 66:11238–11246. [PubMed: 17114237]

Lindahl P, Johansson BR, Leveen P, Betsholtz C. Pericyte loss and microaneurysm formation in PDGF-B-deficient mice. Science. 1997; 277:242–245. [PubMed: 9211853]

Lindahl P, Betsholtz C. Not all myofibroblasts are alike: revisiting the role of PDGF-A and PDGF-B using PDGF-targeted mice. Curr Opin Nephrol Hypertens. 1998; 7:21–26. [PubMed: 9442358]

MacFadyen J, Savage K, Wienke D, Isacke C. Endosialin is expressed on stromal fibroblasts and CNS pericytes in mouse embryos and is down-regulated during development. Gene Expr Patterns. 2007; 7:363–369. [PubMed: 16965941]

Maciag P, Seavey M, Pan Z, Ferrone S, Paterson Y. Cancer immunotherapy targeting the high molecular weight melanoma-associated antigen protein results in a broad antitumor response and reduction of pericytes in the tumor vasculature. Cancer Res. 2008; 68:8066–8075. [PubMed: 18829565]

Makagiansar I, Williams S, Dahlin-Huppe K, Fukushi J, Mustelin T, Stallcup WB. Phosphorylation of NG2 proteoglycan by protein kinase C-α regulates polarized membrane distribution and cell motility. J Biol Chem. 2004; 279:55262–55270. [PubMed: 15504744]

Makagiansar I, Williams S, Mustelin T, Stallcup WB. Differential phosphorylation of NG2 proteoglycan by ERK and PKCα helps balance cell proliferation and migration. J Cell Biol. 2007; 178:155–165. [PubMed: 17591920]

Nehls V, Denzer K, Drenckhahn D. Pericyte involvement in capillary sprouting during angiogenesis in situ. Cell Tiss Res. 1992; 270:469–474.

Nishiyama A, Stallcup WB. Expression of NG2 proteoglycan causes retention of type VI collagen on the cell surface. Mol Biol Cell. 1993; 4:1097–1108. [PubMed: 8305732]

Ozerdem U, Grako KA, Dahlin-Huppe K, Monosov E, Stallcup WB. The NG2 proteoglycan is expressed exclusively by mural cells during vascular morphogenesis. Devel Dynam. 2001; 222:218–227.

Ozerdem U, Monosov E, Stallcup WB. NG2 proteoglycan expression by pericytes in pathological microvasculature. Microvasc Res. 2002; 63:129–134. [PubMed: 11749079]

Ozerdem U, Stallcup WB. Early contribution of pericytes to angiogenic sprouting and tube formation. Angiogenesis. 2003; 6:241–249. [PubMed: 15041800]

Ozerdem U, Stallcup WB. Pathological angiogenesis is reduced by targeting pericytes via the NG2 proteoglycan. Angiogenesis. 2004; 7:269–276. [PubMed: 15609081]

Ozerdem U. Targeting of pericytes diminishes neovascularization and lymphangiogenesis in prostate cancer. The Prostate. 2006a; 66:294–304. [PubMed: 16245280]

Ozerdem U. Targeting pericytes diminishes neovascularization in orthotopic uveal melanoma in NG2 proteoglycan knockout mouse. Ophthalmic Res. 2006b; 38:251–254. [PubMed: 16888406]

Plate KH, Risau W. Angiogenesis in malignant gliomas. Glia. 1995; 15:339–347. [PubMed: 8586468]

Redmer D, Doraiswamy V, Bortnem B, Fisher K, Jabloka-Shariff A, Grazul-Bilska, Reynolds L. Evidence for a role of capillary pericytes in vascular growth of the developing ovine corpus luteum. Biol Reprod. 2001; 65:879–889. [PubMed: 11514354]

Roskelley C, Bissell M. The dominance of the microenvironment in breast and ovarian cancer. Semin Cancer Biol. 2002; 12:97–104. [PubMed: 12027581]

Rubin J. Only in congenial soil: the microenvironment in brain tumorigenesis. Brain Pathol. 2009; 19:144–149. [PubMed: 19076779]

Schlingemann R, Rietvold F, De Wall K, Ferrone S, Ruiter D. Expression of the high molecular weight associated antigen by pericytes during angiogenesis and in healing wound. Am J Pathol. 1990; 136:1393–1405. [PubMed: 1694058]

Schlingemann RO, Oosterwijk E, Wesseling P, Rietveld F, Ruiter D. Aminopeptidase A is a constituent of activated pericytes in angiogenesis. J Pathol. 1996; 179:436–442. [PubMed: 8869294]

Schrappe DM, Klier FG, Spiro R, Waltz T, Reisfeld R, Gladson C. Correlation of chondroitin sulfate proteoglycan expression on proliferating brain capillary endothelial cells with the malignant phenotype of astroglial cells. Cancer Res. 1991; 51:4986–4993. [PubMed: 1893386]

Seyfried NT, Huysentruyt LC, Atwood JA, Xia Q, Seyfried TN, Orlando R. Up-regulation of NG2 proteoglycan and interferon-induced transmembrane proteins 1 and 3 in mouse astrocytoma: a membrane proteomics approach. Cancer Lett. 2008; 263:243–252. [PubMed: 18281150]

Shibuya M. Brain angiogenesis in developmental and pathological processes: therapeutic aspects of vascular endothelial growth factor. FEBS J. 2009; 276:4636–4643. [PubMed: 19664071]

Shoshan Y, Nishiyama A, Chang A, Mork S, Barnett G, Cowell J, Trapp B, Staugaitis S. Expression of oligodendrocyte progenitor cell antigens by gliomas: implications for the histogenesis of brain tumors. Proc Natl Acad Sci USA. 1999; 96:10361–10366. [PubMed: 10468613]

Simonavicius N, Robertson D, Bax D, Jones C, Huijbers I, Isacke C. Endosialin (CD248) is a marker of tumor-associated pericytes in high-grade glioma. Mod Pathol. 2008; 21:308–315. [PubMed: 18192970]

Sloan A, Nock C, Einstein D. Diagnosis and treatment of melanoma brain metastasis: a literature review. Cancer Control. 2009; 16:248–255. [PubMed: 19556965]

Song S, Ewald A, Stallcup WB, Werb Z, Bergers G. PDGFRβ+ perivascular progenitor cells in tumours regulate pericyte differentiation and vascular survival. Nature Cell Biol. 2005; 7:870–879. [PubMed: 16113679]

Stallcup WB, Dahlin K, Healy P. Interaction of the NG2 chondroitin sulfate proteoglycan with type VI collagen. J Cell Biol. 1990; 111:3177–3188. [PubMed: 2269670]

Stallcup WB, Huang FJ. A role for the NG2 proteoglycan in glioma progression. Cell Adhesion and Migration. 2008; 2:192–201. [PubMed: 19262111]

Tigges U, Hyer E, Scharf J, Stallcup WB. FGF2-dependent neovascularization of subcutaneous Matrigel plugs is initiated by bone marrow-derived pericytes and macrophages. Development. 2008; 135:523–532. [PubMed: 18171688]

Tillet E, Ruggiero F, Nishiyama A, Stallcup WB. The membrane-spanning proteoglycan NG2 binds to collagens V and VI through the central non-globular domain of its core protein. J Biol Chem. 1997; 272:10769–10776. [PubMed: 9099729]

Tillet E, Gential B, Garrone R, Stallcup WB. NG2 proteoglycan mediates β1 integrin-independent cell adhesion and spreading on collagen VI. J Cell Biochem. 2002; 86:726–736. [PubMed: 12210739]

Van der Valk P, Lindeman J, Kamphorst W. Growth factor profiles in human gliomas. Do non-tumor cells contribute to tumor growth in glioma? Ann Oncol. 1997; 8:1023–1029. [PubMed: 9402177]

Virgintino D, Girolamo F, Errede M, Capobianco C, Robertson D, Stallcup WB, Perris R, Roncali L. A intimate interplay between precocious, migrating pericytes and endothelial cells governs human fetal brain angiogenesis. Angiogenesis. 2007; 10:35–45. [PubMed: 17225955]

Wesseling P, Schlingemann R, Rietveld F, Burger P, Ruiter D. Early and extensive contribution of pericytes/vascular smooth muscle cells to microvascular proliferation in glioblastoma multiforme. J Neuropathol Exp Neurol. 1995; 54:304–310. [PubMed: 7745429]

Yuan L, Siegel M, Choi K, Khosla C, Miller C, Jackson E, Piwnica-Worms D, Rich K. Transglutaminase 2 inhibitor KCC009 disrupts fibronectin assembly in the extracellular matrix

and sensitizes orthotopic gliomas to chemotherapy. Oncogene. 2007; 26:2563–2573. [PubMed: 17099729]

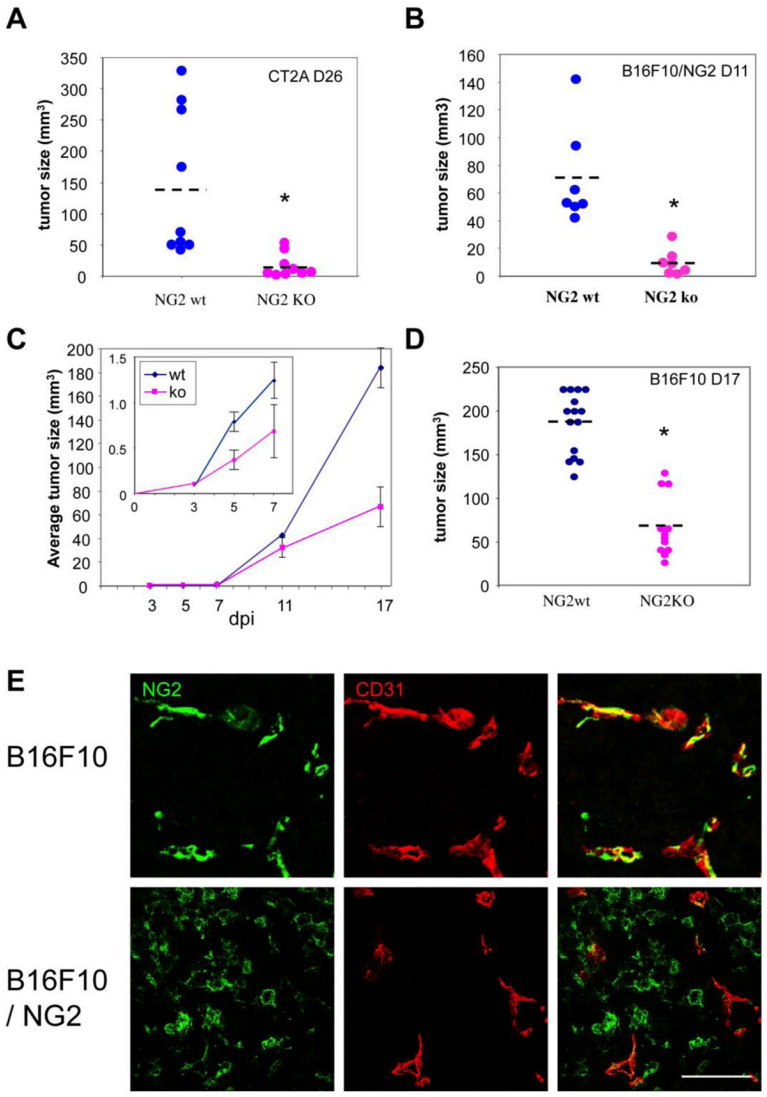

Figure 1. CT2A, B16F10, and B16F10/NG2 tumors in wild type and NG2 null mouse brain

Tumor sizes were measured in wild type and NG2 null mice that had been injected in the corpus callosum with 1×10^4 CT2A, B16F10/NG2, or B16F10 cells. (A) Nine wild type and nine NG2 null mice were injected with CT2A cells and analyzed for tumor size at 26 days post-injection. On average, CT2A tumors in NG2 null mice are 7-fold smaller than in wild type mice. (B) Seven wild type and seven NG2 null mice were injected with B16F10/NG2 cells and analyzed for tumor size at 11 days post-injection. The average tumor size was 10-fold smaller in NG2 null mice. (C) Five mice in each group were analyzed at days 3, 5, 7, 11, and 17 after injection of B16F10 cells. Average tumor sizes are plotted versus days post-injection. The inset panel shows the first week after tumor initiation on an expanded scale, revealing that tumors in wild type and NG2 null mice begin to diverge in size between 3 and 7 days post-injection. (D) Fifteen mice in each group were analyzed at 17 days after injection of B16F10 cells. B16F10 tumors in NG2 null mice are at least 3-fold smaller than in wild type mice. Dashed lines show average tumor sizes. * $P<0.001$. (E) Double immunostaining for NG2 (green) and CD31 (red) shows that in both B16F10 and B16F10/NG2 tumors, NG2 is expressed by pericytes associated with CD31-positive endothelial cells.

Apart from the vasculature, NG2 is also strongly expressed by B16F10/NG2 tumor cells, but is absent from B16F10 tumor cells. Bar = 100 μm.

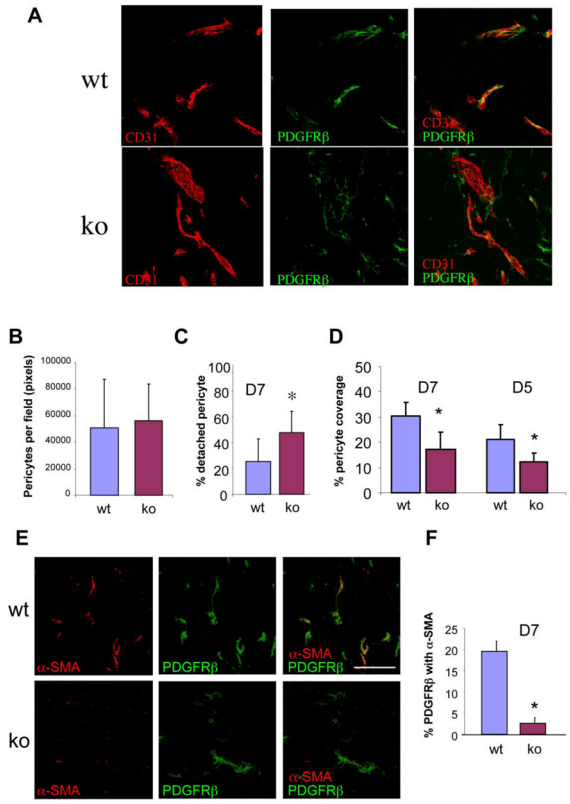

Figure 2. Pericyte investment of tumor blood vessels and pericyte maturation

(A) To assess pericyte investment of blood vessels, sections of B16F10 tumor-bearing wild type (wt) and NG2 null (ko) brains at 7 days post-injection were double-stained for CD31 and PDGFRβ. Confocal z-stacks of images were processed by image analysis to quantify several aspects of the relationship between endothelial cells (red) and pericytes (green). Bar = 100 μm. Data in panels B-D are derived from 4 independent tumors of each genotype, sampling 4 fields from 3 sections in each tumor (12 fields × 4 tumors). (B) Quantification of green pixels allowed a comparison of the total number of pericytes per field. (C) The extent to which pericytes were not associated with endothelial tubes (detached pericytes) was assessed by quantifying the percentage of green pixels not in physical contact with red pixels. (D) The extent of pericyte ensheathment of endothelial cells was determined by quantifying the percentage of red pixels that were covered by green pixels. These values were determined both at day 5 and day 7 of tumor growth, revealing a deficit in the NG2 null mouse at both days.

* $P<0.01$. (E) To evaluate pericyte maturation in tumor blood vessels, sections of 7-day tumors were stained for CD31 to visualize blood vessels (not shown), and for PDGFRβ (green) and αSMA (red) to identify nascent and maturing pericytes, respectively. (F) Data in panel F are derived from 4 independent tumors for each genotype, sampling 4 fields from 3 sections in each tumor. Confocal z-stacks of images were processed by image analysis to quantify the extent to which the PDGFRβ label is coincident with αSMA. Bar = 100 μm. * $P < 0.0003$

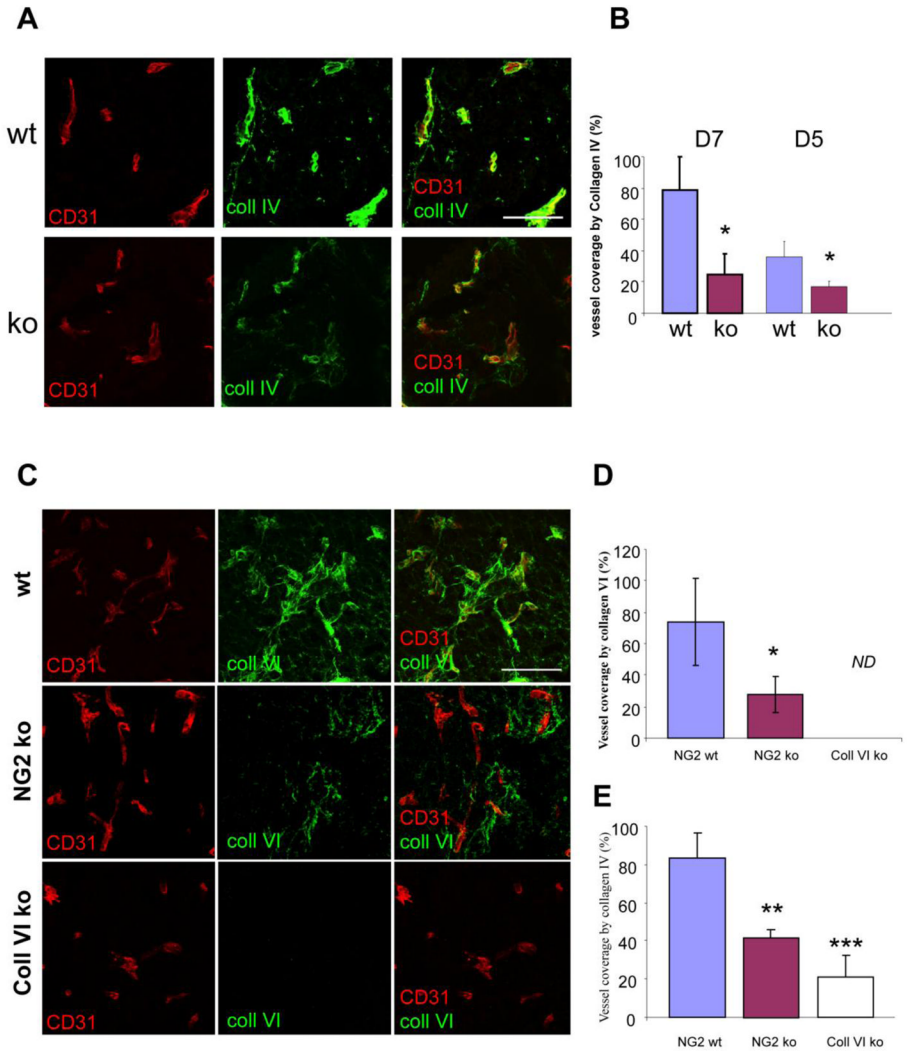

Figure 3. Basal lamina deposition in tumor blood vessels

(A) To evaluate basal lamina assembly associated with blood vessels, sections of 7-day tumors were double-stained for CD31 (red) and collagen IV (green). Bar = 100 μm. (B) Data in panel B are derived from 3 independent tumors for each genotype, sampling 4 fields from 3 sections in each tumor. Both day 5 and day 7 tumors were analyzed. Confocal z-stacks of images were processed by image analysis to quantify the extent to which collagen IV labeling overlapped with CD31 labeling. Basal lamina deposition is reduced in the NG2 null mouse at both time points. * $P < 0.002$. (C) Association of collagen VI with 7-day tumor blood vessels was evaluated in wild type (wt), NG2 null (NG2 ko), and collagen VI null (coll VI ko) mice by double-staining for CD31 (red) and collagen VI (green). Bar = 100 μm. (D) Data in panel D are derived from 3 tumors for each genotype, sampling 4 fields from 3 sections in each tumor. Image analysis of z-stacks of confocal images allowed determination of the percentage of CD31 pixels covered by collagen VI pixels. * $P<0.03$. ND, not detectable. (E) Assembly of collagen IV-positive basal lamina was compared in tumor vessels in wild type, NG2 null, and collagen VI null mice. ** $P < 0.007$ *** $P < 0.002$

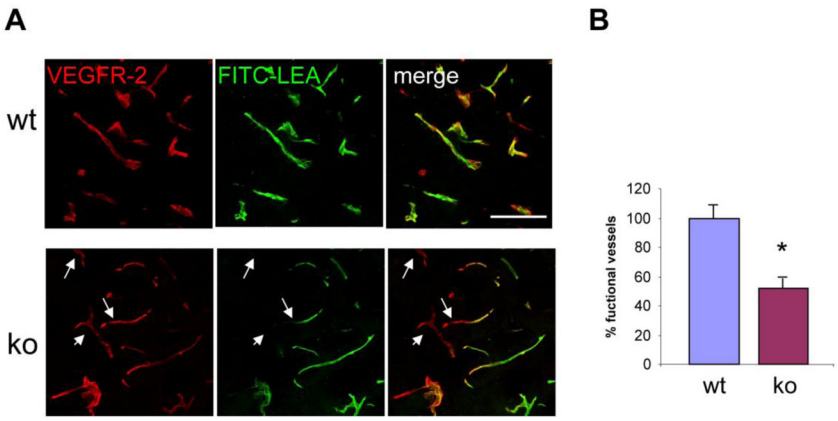

Figure 4. Patency of tumor vessels

(A) Patency of 7-day tumor vessels was determined following intravenous injection of FITC-LEA lectin (green), followed by perfusion to clear unbound lectin. Sections were then stained for VEGFR-2 (red) to allow comparison of the total number of blood vessels with the number of patent vessels. Arrows denote VEGFR-2-positive vessels without LEA lectin labeling. Bar = 100 μm. (B) Data in panel B are derived from 4 independent tumors for each genotype, sampling 4 fields in 3 sections in each tumor. Image analysis of z-stacks of confocal images allowed determination of the percentage of VEGFR-2 pixels covered by LEA lectin pixels. * P<0.001.

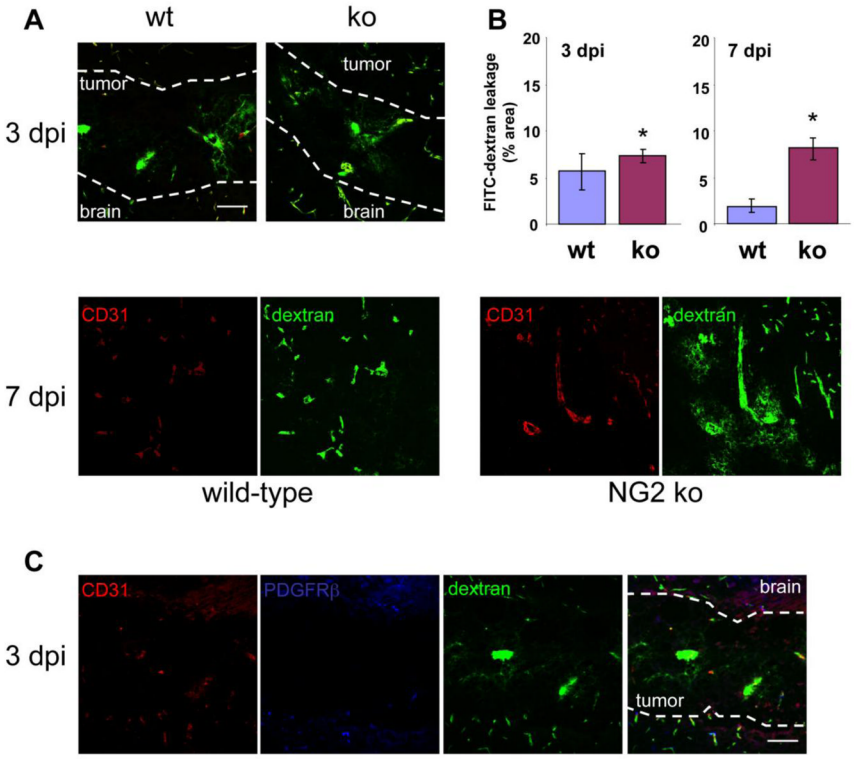

Figure 5. Leakiness of tumor vessels

(A) Leakiness of tumor vessels at 3 (top panels) and 7 (lower panels) days post-injection (dpi) was visualized by intravenous injection of FITC-dextran (green) followed by a 10-minute circulation period and tissue fixation. Sections were stained for CD31 (red) to define blood vessel boundaries. Dashed lines show the brain-tumor boundaries at 3 dpi. Bar = 100 μm. z-stacks of confocal images were processed by image analysis to quantify FITC-dextran pixels lying external to CD31-positive vessels. (B) Data in panel B are derived from 3 independent tumors for each genotype, sampling 4 fields in 3 sections from each tumor. The extravascular FITC-dextran area is expressed as the percentage of the total tumor area at 3 dpi (left panel) and 7 dpi (right panel). * $P<0.001$. (C) Pericyte investment of tumor vessels in wild type mice at 3 days post-injection was evaluated by double-staining for CD31 (red) and PDGFRβ (blue) in sections from FITC-dextran-perfused (green) tumors at 3 dpi. Dashed lines mark brain-tumor boundaries. Bar = 100 μm.

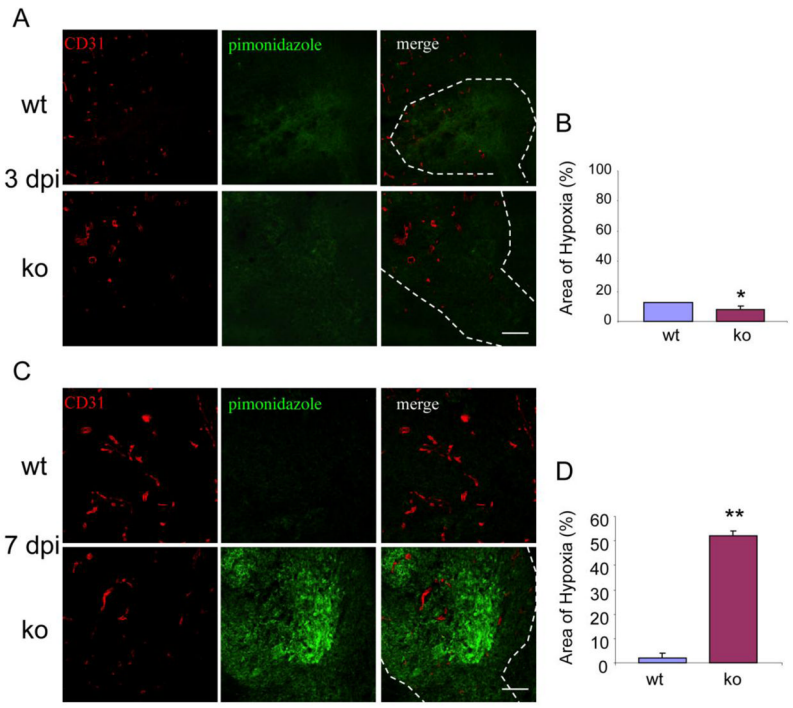

Figure 6. Levels of tissue hypoxia in tumors

Tissue sections were prepared from animals that had been injected with pimonidazole hypoxia probe at 3 (A) and 7 days (C) of tumor development. Sections were double-stained for pimonidazole (green) and CD31 (red). Data in panels B and D were derived from 3 independent tumors for each genotype, sampling 4 fields in 3 sections from each tumor. Hypoxia levels at 3 (B) and 7 (D) dpi were determined as the percentage of total tumor area covered by pimonidazole pixels. Dashed lines illustrate brain-tumor boundaries. * $P = 0.192$, ** $P<0.0001$. Bar = 100 μm.